Facile Route to Synthesize Large-Mesoporous γ-Alumina by Room Temperature Ionic Liquids

HoSeok Park,[†] Seong Ho Yang,[‡] Young-Si Jun,[†] Won Hi Hong,*[,†] and Jeung Ku Kang[‡]

Department of Chemical and Biomolecular Engineering and Department of Materials Science and Engineering, KAIST, Guseong-dong 373-1, Yusong-gu, Daejeon, Republic of Korea

Received September 3, 2006. Revised Manuscript Received November 19, 2006

A large mesoporous γ-alumina was fabricated through a thermal process without postaddition of molecular or organic solvents at ambient pressure in an open container by using the dual functions of 1-hexadecyl-3-methylimidazolium chloride (C_{16}MimCl) as room-temperature ionic liquids (RTILs), i.e., templating and cosolvent functions. In this synthesis, a thermal process with the assistance of RTILs was the key technology for induction of the nanostructure of aluminum hydroxide and transformation to boehmite crystallites by means of intermolecular interaction. Both C_{16}MimCl/boehmite hybrid and γ-alumina displayed the nanostructure consisting of randomly debundled nanofibers embedded in wormlike porous networks. Nanofibers of C_{16}MimCl/boehmite hybrid and γ-alumina exhibited a length of ca. 40−60 nm and a diameter of ca. 1.5−3 nm. In particular, γ-alumina had good thermal stability and reasonable acidic sites. After conversion from boehmite crystallites into γ-phase by calcination, this nanostructured γ-alumina obtained the largest surface area and pore volume among large mesoporous γ-aluminas around 10 nm pore size, i.e., 470 $m^2\ g^{-1}$ in surface area, 1.46 $cm^3\ g^{-1}$ in pore volume, and 9.9 nm in pore size by calcination at 550 °C. Therefore, this synthetic method is a facile way to synthesize various nanostructured inorganic materials with the enhanced physical properties.

1. Introduction

Room-temperature ionic liquids (RTILs) have received much attention as a functional material offering a wide range of possibilities for applications in solvents,[1a] catalysis,[1a,b] electrochemistry,[1c] separation,[1d] etc.[1e] RTILs, which are composed of large organic cation and weakly coordinating anion, can be novel solvents that have nonvolatility and tailorable solubility as a result of the appropriate combination of anion and cation components.[1a] Lyotropic and thermotropic behavior are controlled by a length of alkyl chain of cation, while hydrophilicity and the strength of hydrogen bonding are determined by the types of anion.[2] Recently, the new solvent system of RTILs makes possible their use as a reaction medium, resulting in the transformation to the construction of nanostructured materials facilitated by driving forces such as microwaves.[3] In addition to potential applications of RTILs as solvents, they are used as soft templates to fabricate the nanostructured materials.[4] There have been very few reports, however, describing the solvent or template action of RTILs to promote the formation of nanostructured inorganic materials. Herein, we report the first attempt to the fabrication of γ-alumina by using RTILs, thereby inducing its nanostructure, large mesopore, and crystallization into boehmite phase.

γ-Alumina, which is formed upon the dehydration of boehmite at temperature ranging from 350 to 1000 °C,[5c] is known to be the advanced material that is considered attractive for applications of adsorbent, catalyst, and catalyst support due to its thermal, chemical, and mechanical stabilities as well as catalytic and textural characteristics.[5] In recent years, many efforts have concentrated on the development of nanostructured materials consisting of inorganic oxides rather than organic compounds[6] because the formation of

* Corresponding author. Tel.: +82-42-869-3959. Fax: +82-42-869-3910. E-mail: whhong@kaist.ac.kr.

[†] Department of Chemical and Biomolecular Engineering.

[‡] Department of Materials Science and Engineering.

(1) (a) Welton, T. *Chem. Rev.* **1999**, *99*, 2071−2083. (b) Dupont, J.; de Souza, R. F.; Suarez, P. A. Z. *Chem. Rev.* **2002**, *102*, 3667−3692. (c) Buzzeo, M. C.; Evans, R. G.; Compton, R. G. *Chem. Phys. Chem.* **2004**, *5*, 1107−1120. (d) Blanchard, L. A.; Hancu, D.; Beckman, E. J.; Brennecke, J. F. *Nature* **1999**, *399*, 28−29. (e) Fei, Z.; Geldbach, T. J.; Zhao, D.; Dyson, P. J. *Chem. Eur. J.* **2006**, *12*, 2122−2130.

(2) (a) Bleasdale, T. A.; Tiddy, G. J. T.; Wyn-Jones, E. *J. Phys. Chem.* **1991**, *95*, 5385−5386. (b) Neve, F.; Francescangeli, O.; Crispini, A. *Inorg. Chim. Acta* **2002**, *338*, 51−58. (c) Anthony, J. L.; Maginn, E. J.; Brennecke, J. F. *J. Phys. Chem. B* **2001**, *105*, 10942−10949.

(3) (a) Zhu, Y. J.; Wang, W. W.; Qi, R. J.; Hu, X. L. *Angew. Chem., Int. Ed.* **2004**, *43*, 1410−1414. (b) Jiang, Y.; Zhu, Y. J. *J. Phys. Chem. B* **2005**, *109*, 4361−4364. (c) Xu, Y. P.; Tian, Z. J.; Wang, S. J.; Hu, Y.; Wang, L.; Wang, B. C.; Ma, Y. C.; Hou, L.; Yu, J. Y.; Lin, L. W. *Angew. Chem., Int. Ed.* **2006**, *45*, 3965−3970. (d) Jacob, D. S.; Bitton, L.; Grinblat, J.; Felner, I.; Koltypin, Y.; Gedanken, A. *Chem. Mater.* **2006**, *18*, 3162−3168.

(4) (a) Firestone, M. A.; Dietz, M. L.; Seifert, S.; Trasobares, S.; Miller, D. J.; Zaluzec, N. J. *Small* **2005**, 754−760. (b) Liu, Y.; Wang, M.; Li, Z.; Liu, H.; He, P.; Li, J. *Langmuir* **2005**, *21*, 1618−1622. (c) Cooper, E. R.; Andrews, C. D.; Wheatley, P. S.; Webb, P. B.; Wormald, P.; Morris, R. E. *Nature* **2004**, *430*, 1012−1016. (d) Lee, B.; Luo, H.; Yuan, C. Y.; Lin, J. S.; Dai, S. *Chem. Commun.* **2004**, 240−241. (e) Zhu, Y. J.; Wang, W. W.; Qi, R. J.; Hu, X. L. *Angew. Chem., Int. Ed.* **2004**, *43*, 1410−1414.(f) Zhou, Y.; Schattka, J. H.; Antonietti, M. *Nano Lett.* **2004**, *4*, 477−481.

(5) (a) Zhang, Z.; Pinnavaia, T. J. *J. Am. Chem. Soc.* **2002**, *124*, 12294−12301. (b) Zhang, Z.; Hicks, R. W.; Pauly, T. R.; Pinnavaia, T. J. *J. Am. Chem. Soc.* **2002**, *124*, 1592−1593. (c) Zhang, W.; Pinnavaia, T. J. *Chem. Commun.* **1998**, 1185−1186. (c) Trueba, M.; Trasatti, S. P. *Eur. J. Inorg. Chem.* **2005**, *17*, 3393−3403. (d) Hicks, R. W.; Pinnavaia, T. J. *Chem. Mater.* **2003**, *15*, 78−82.

(6) (a) Xiong, Y.; Mayeres, B. T.; Xia, Y. *Chem. Commun.* **2005**, *40*, 5013−5022. (b) Kolmakov, A.; Moskovits, M. *Annu. Rev. Mater. Res.* **2004**, *34*, 151−180.

10.1021/cm0620887 CCC: $37.00
Published on Web 01/05/2007

these inorganic nanostructures is challenging from a pure scientific point of view and these materials also have great potential for applications in a large variety of fields.[7] Nevertheless, it is difficult to synthesize mesoporous γ-alumina and induce its nanostructure compared to that of silica or titania, due to the fast reaction rates of aluminum alkoxides and harsh synthetic conditions.[8] Solution syntheses such as hydro(or solvo)thermal synthesis and soft-template method have been commonly used to fabricate the nanostructured boehmite or γ-alumina without any additive to control the rate of hydrolysis.[9] In the case of hydrothermal synthesis, high pressure and temperature are required to direct specific nanostructure and trigger transformation from amorphous to crystalline phase. Although soft-template synthesis can form the nanostructure of γ-alumina under mild conditions, it also needs the assistance of additional volatile organic or molecular solvent in a closed container. Therefore, RTILs used during subsequent heating can be strong candidates for fabricating the nanostructured γ-alumina under mild conditions without rate-controlling agents, as this synthetic method has some advantages over general solution syntheses in points of eliminating the complications associated with high hydrothermal pressures in a sealed autoclave and avoiding the postaddition of organic solvents. RTILs instead of organic or molecular solvent were used as cosolvent as well as template agents during thermal treatment in an open container. In this manuscript, we synthesized a large mesoporous γ-alumina with good textural and physical properties, by means of the dual functions of RTILs, i.e., templating and cosolvent functions, via a thermal process.

2. Experimental Section

Materials. All chemicals used were analytical grade and used without further purification. 1-Hexadecyl-3-methylimidazolium chloride (C_{16}MimCl, high purity 99.9%) was supplied by C-TRI. Aluminum tri-*sec*-butoxide (Aldrich, 99.9%) was used as aluminum precursor without further purification. 1-Propanol and hydrochloric acid (HCl) were supplied by Aldrich.

Synthesis of Nanostructured γ-Alumina. C_{16}MimCl (0.911 g) was mixed with 4 mL of 1-propanol and 0.309 mL of deionized water. After 0.3 mL of an aqueous solution of 0.01 M HCl, which serves as an acid catalyst, was added to the mixture dropwise, the pH of transparent solution was 5.5. After 1.309 g of aluminum tri-*sec*-butoxide was added to a transparent mixture, the pH of translucent solution reached 10.1. 1-Propanol and water were used to hydrolyze and condense aluminum precursors. The resultant mixture was stirred at 60 °C for 120 min, followed by aging at 60 °C for 1 day. To complete gelation and induce the formation of boehmite structure, the mixture was heated to 120 °C for 2 days at ambient pressure. RTILs were removed by calcination at 300, 550, 700, and 800 °C for 2 h, after heating at a rate of 2 °C/min from room temperature to 300, 550, 700, and 800 °C, respectively.

Characterization. Elemental analysis was performed within the accuracy of 0.3% by elemental analyzer, which is EA1110-FISONS, manufactured by ThermoQuest Italia S.P.A (CE INSTRUMENTS). C, H, O, and N elements of all samples were analyzed quantitatively in the range of 0.01−100%. TEM images were collected on an E.M. 912Ω energy-filtering transmission electron microscope (EF TEM, 120 kV) and a JEM-3010 high-resolution transmission electron microscope (HR TEM, 300 kV). With a counting time of 2 h, small-angle X-ray scattering (SAXS) data were gathered on a Rigaku D/max-2500 (5 kW) with an image plate system equipped with a Cu Kα radiation generator. X-ray diffraction (XRD) data were obtained on a Rigaku D/max llC (3 kW) with a θ/θ goniometer equipped with a Cu Kα radiation generator. The diffraction angle of the diffractograms was in the range of $2\theta = 10-80°$. FT-IR ATR spectra were collected on a JASCO FT-IR 470 plus as attenuated total reflection. Each spectrum, which was recorded as the average of 12 scans with a resolution of 4 cm^{-1}, was collected from 4000 to 650 cm^{-1}.^{27}Al nuclear magnetic resonance (NMR) spectra were obtained by using a 400 MHz solid-state NMR spectrometer (Bruker, DSX 400) with CP/MAS probe. Thermogravimetric analyses (TGA) were carried out using a Dupont 2200 thermal analysis station. Every sample was heated from 30 to 900 °C at a rate of 10 °C/min under a nitrogen atmosphere. N_2 sorption/desorption data was obtained using a gas sorption analyzer (NOVA 4200 Ver. 7.10). The specific surface area was calculated by the BET equation and pore size was determined by the BJH model.

3. Results and Discussion

Morphology of C_{16}MimCl/Boehmite Hybrid and γ-Alumina. Scheme 1 illustrates the synthetic process of the nanostructured large mesoporous γ-alumina via a thermal process by using C_{16}MimCl as RTILs. In conventional solution syntheses, the nanostructures of inorganic materials are induced by hydro(or solvo)thermal treatment or assistance of additional organic solvents in a sealed autoclave.[9] In contrast, the key step in this synthetic method to fabricate the nanostructured γ-alumina was the thermal process with the assistance of RTILs in an open container at ambient pressure. TEM images in Figures 1a and 1b present the morphology of C_{16}MimCl/boehmite hybrid and γ-alumina prepared by RTILs. Both C_{16}MimCl/boehmite hybrid and γ-alumina had the nanostructure consisting of randomly debundled nanofibers embedded in wormlike porous networks. Nanofibers of C_{16}MimCl/boehmite hybrid displayed a length of ca. 40−60 nm and a diameter of ca. 1.5−3 nm, exhibiting a similar geometry to a fibrious or hierarchical γ-alumina fabricated by block copolymer template.[9c,g] After conversion from boehmite phase into γ-phase by calcination, the nanostructure of C_{16}MimCl/boehmite hybrid was conserved. The complete removal of C_{16}MimCl was confirmed by evaluating the content of carbon and nitrogen of calcined aluminas by means of element analysis. Figure 1c shows that the wormlike motif of γ-alumina induced broad SAXS peaks attributed to

(7) van Bommel, K. J. C.; Friggeri, A.; Shinkai, S. *Angew. Chem., Int. Ed.* **2003**, *42*, 980−999.
(8) Cabrera, S.; Haskouri, J. E.; Alamo, J.; Beltrán, A.; Beltrán, D.; Mendioroz, S.; Marcos, M. D.; Amorós, P. *Adv. Mater.* **1999**, *11*, 379−381.
(9) (a) Zhu, H. Y.; Gao, X. P.; Song, D. Y.; Bai, Y. Q.; Ringer, S. P.; Gao, Z.; Xi, Y. X.; Martens, W.; Riches, J. D.; Frost, R. L. *J. Phys. Chem. B* **2004**, *108*, 4245−4247. (b) Kuang, D.; Fang, Y.; Liu, H.; Frommen, C.; Fenske, D. *J. Mater. Chem.* **2003**, *13*, 660−662. (c) Zhu, H. Y.; Riches, J. D.; Barry, J. C. *Chem. Mater.* **2002**, *14*, 2086−2093. (d) Lee, H. C.; Kim, H. J.; Rhee, C. H.; Lee, K. H.; Lee, J. S.; Chung, S. H. *Microporous Mesoporous Mater.* **2005**, *79*, 61−68. (e) Lee, H. C.; Kim, H. J.; Chung, S. H.; Lee, K. H.; Lee, H. C.; Lee, J. S. *J. Am. Chem. Soc.* **2003**, *125*, 2882−2883. (f) Kim, H. J.; Lee, H. C.; Rhee, C. H.; Chung, S. H.; Lee, H. C.; Lee, K. H.; Lee, J. S. *J. Am. Chem. Soc.* **2003**, *125*, 13354−13355. (g) Bronstein, L. M.; Chernyshov, D. M.; Karlinsey, R.; Zwanziger, J. W.; Valentina, G.; Matveeva, V. G.; Sulman, E. M.; Demidenko, G. N.; Hentze, H. P.; Antonietti, M. *Chem. Mater.* **2003**, *15*, 2623−2631. (f) Tang, B.; Ge, J.; Zhuo, L.; Wang, G.; Niu, J.; Shi, Z.; Dong, Y. *Eur. J. Inorg. Chem.* **2005**, *21*, 4366−4369.

Scheme 1. Illustration for the Synthesis Process of Large Mesoporous γ-Alumina with Nanostructure Prepared by the Dual Functions of 1-Hexadecyl-3-methylimidazolium Chloride, C_{16}MimCl

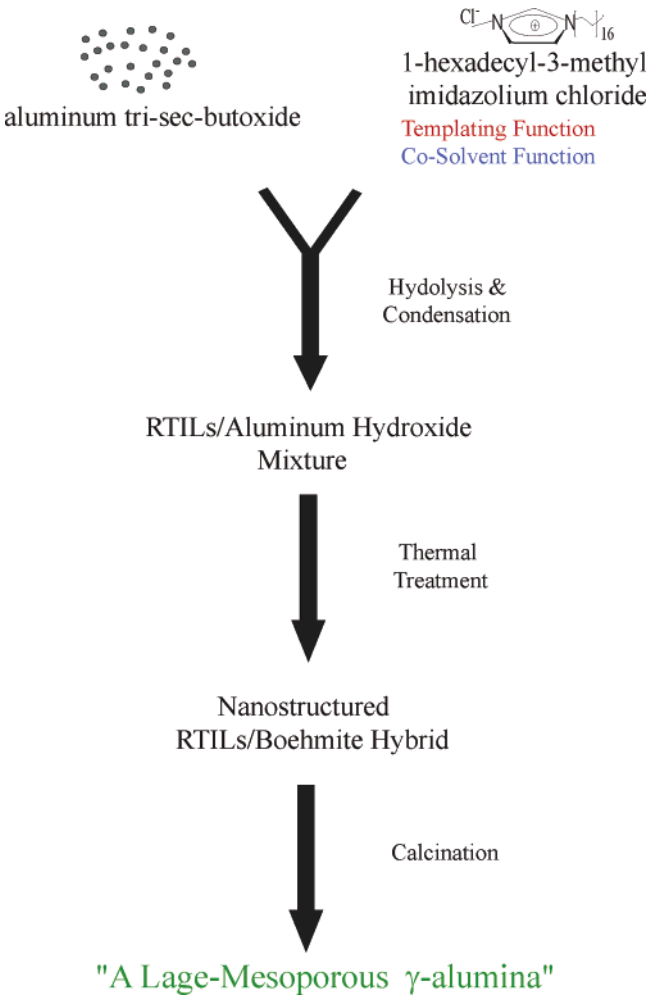

disordered porous structure and large pore size. In addition, after calcination at 800 °C, broad SAXS peak of γ-alumina disappeared completely. Figure 1d shows that the phase transformation was identified by XRD patterns of the C_{16}MimCl/boehmite hybrid and γ-alumina obtained by calcination at 800 °C. The peaks of uncalcined samples were ascribed to the crystalline boehmite phase, whereas those of calcined samples were attributed to transitional γ-alumina phase. SAED patterns superimposed with diffused rings also reflected the existence of crystalline boehmite and γ-alumina phases.

Formation of Nanostructured γ-Alumina by Templating and Cosolvent Functions of C_{16}MimCl. To clarify the effect of thermal treatment on the formation of nanostructure, γ-alumina was fabricated without thermal treatment under the same condition as γ-alumina prepared by C_{16}MimCl. For the absence of a thermal process, wormlike mesoporous structure of γ-alumina is observed by the TEM image in Figure 2a, indicating that a thermal process was the key route for fabricating the nanostructured γ-alumina. In the case of boehmite and γ-alumina fabricated without C_{16}MimCl under the same experimental condition as this synthetic process, both relatively low crystallinity and indiscernible shape were observed by TEM and XRD as shown in Figures 2b and 2d. Under this synthetic condition, C_{16}MimCl played a crucial role of template in forming the nanostructure of γ-alumina. For the purpose of verifying templating and cosolvent functions of C_{16}MimCl more clearly during subsequent heating, the construction of nanostructured γ-alumina was observed by TEM and XRD, after removing volatile solvents by evacuation under vacuum before thermal treatment. Figures 2c and 2d show morphology and XRD patterns similar to those of C_{16}MimCl/boehmite hybrid or γ-alumina as indicated in Figure 1. Despite not confirming the complete removal of all volatile solvents such as water and 1-propanol by direct evidence, most of the solvents were evaporated and removed due to their volatility and low boiling point during thermal treatment and evacuation under vacuum. The presence of solvents was verified by the absence of the O−H band around 3200 cm^{-1} in FT-IR spectra, after evacuation under vacuum and thermal treatment. In contrast, C_{16}MimCl, which was removed negligibly owing to its thermal stability and nonvolatility (as evidenced in TGA data below), acted as ionic solvent during subsequent heating.[1a,4c] Thus, C_{16}MimCl acted as the evident dual roles of templating and cosolvent agents in fabricating the nanostrucutred C_{16}MimCl/boehmite hybrid by means of only thermal treatment without post-addition of organic or molecular solvents and high pressure in a sealed autoclave.

The FT-IR spectra and XRD patterns were analyzed to understand the formation process of the nanostructured C_{16}MimCl/boehmite hybrid as shown in Figure 3. Hydrogen bonding can occur at the interface between anions of C_{16}MimCl and building blocks of aluminum hydroxides, as Cl^- anions of C_{16}MimCl include strong hydrophilicity and capability for hydrogen bonding accepting functionality.[2c,10] Therefore, when another hydrogen bond donating species in the surface of boehmite surrounds C_{16}MimCl, hydrogen bonds between the cations and anions of C_{16}MimCl are perturbed.[10b] Three peaks of C_{16}MimCl in the circular region are attributed to the CH···Cl hydrogen bonding between the anions and the 4,5-hydrogens of the imidazolium ring.[11] As a result of perturbation of hydrogen bonding between cations and anions of C_{16}MimCl, the peaks of C_{16}MimCl/aluminum sol before thermal treatment were superimposed or disappeared by O−H bonds, while the peaks of C_{16}MimCl/boehmite were shifted to lower wavenumbers due to less electron density by means of polarization via hydrogen bonding. In the RTILs-templated system, the nanostructures of inorganic oxides were induced by hydrogen bonding-co-π−π stacking mechanism proved by FT-IR spectroscopy as discussed by previous reports.[4f] The reorganizing process of aluminum hydroxide crystallites via π−π stacking as well as hydrogen bonding significantly influenced other peaks related to the imidazolium ring and anion of C_{16}MimCl in the IR spectra. In addition, evidence for the contribution of π−π stacking to self-assembly was also found in the XRD patterns. Additional XRD diffraction peaks with remarkable

(10) (a) Yoshizawa, M.; Xu, W.; Angell, C. A. *J. Am. Chem. Soc.* **2003**, *125*, 15411−15419.(b) Shi, F.; Zhang, Q.; Li, D.; Deng, Y. *Chem.−Eur. J.* **2005**, *11*, 5279−5288. (c) Shi, F.; Deng, Y. *Spectrochim. Acta Part A* **2005**, *62*, 239−244.
(11) Dieter, K. M.; Dymek, C. J., Jr.; Heimer, N. E.; Rovang, J. W.; Wilkes, J. S. *J. Am. Chem. Soc.* **1988**, *110*, 2722−2726.

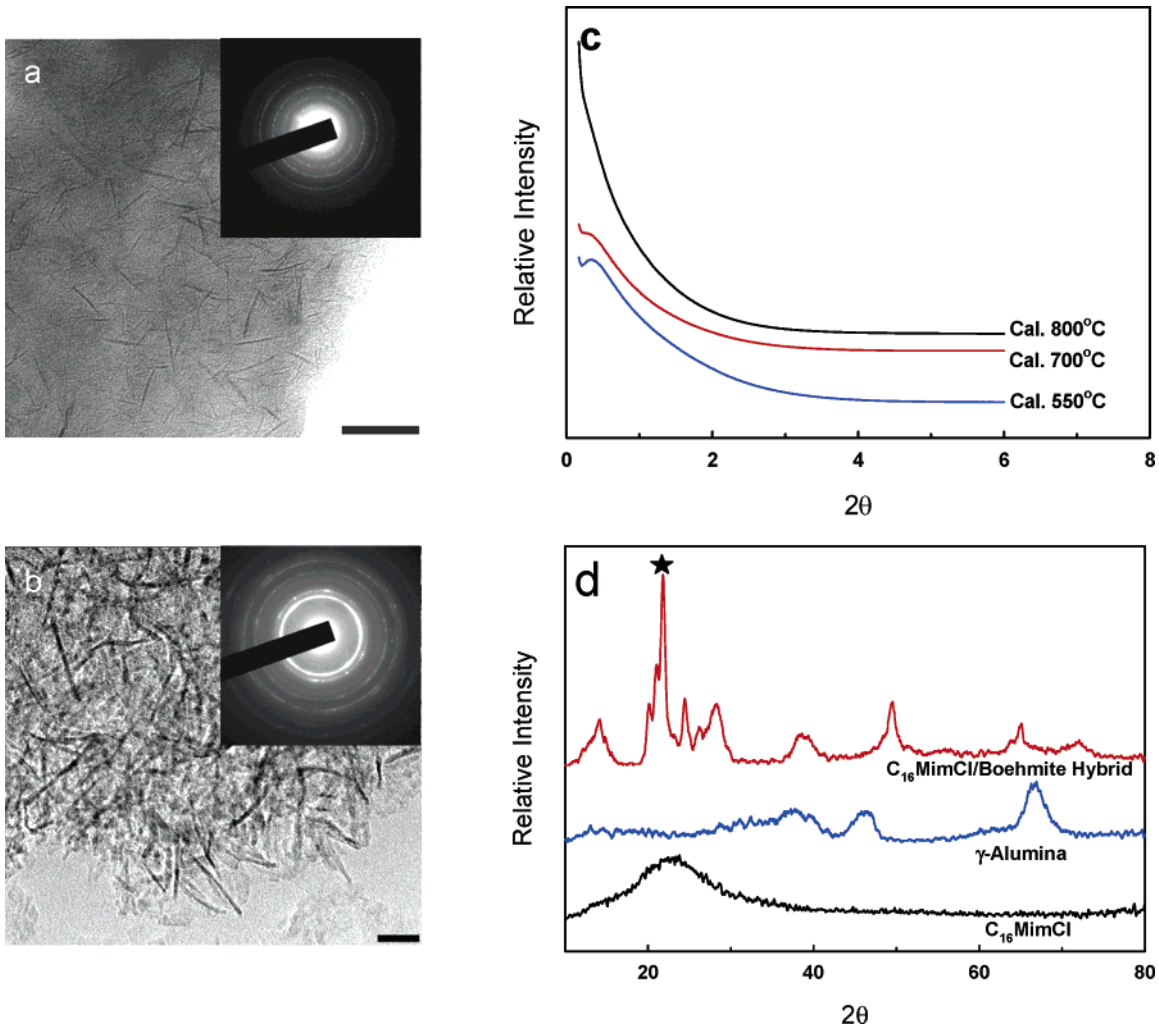

Figure 1. TEM images of (a) C_{16}MimCl/boehmite hybrid (50 nm bar); (b) γ-alumina (20 nm bar) after removal of C_{16}MimCl by calcination at 800 °C. (c) SAXS patterns of γ-aluminas prepared by C_{16}MimCl after calcination at 550, 700, and 800 °C and (d) XRD patterns of pristine C_{16}MimCl, C_{16}MimCl/boehmite hybrid, and γ-alumina after calcination at 800 °C.

intensities around 20°, noted with an asterisk, are unrelated to the crystalline phases of boehmite. The *d* spacing of 4.068 Å is caused by self-ordering of imidazolium rings via $\pi-\pi$ stacking of RTILs, as provided by the single XRD peak of C_{16}MimCl in Figure 1d,[12] suggesting that the shoulder peaks were likely due to the generation of polycrystallites or the splitting of the peak via mutual interaction. Zhu et al. proved that polymer micelles induce the formation of fibrous morphology and the growth of boehmite crystallites through mutual interaction via hydrogen bonding between aluminum hydroxide and template.[9c] In a similar manner to surfactant-induced fiber formation (SIFF) mechanism,[9c] the nanostructure of C_{16}MimCl/boehmite hybrid was formed though hydrogen bonding between C_{16}MimCl and aluminum hydroxide as well as $\pi-\pi$ stacking of imidazolium rings. The changes in the O−H band around 3200 cm^{-1} in FT-IR spectra before and after heat treatment elucidate that as both the transformation of aluminum hydroxide into boehmite phase and the construction of nanostructure were carried out during thermal treatment, the hydrolytic transformation of hydroxyl (Al−OH) centers to oxo (Al−O−Al) bridges reduced the surface charge of the building blocks by squeezing out water molecules, thereby inducing their aggregation and organization.[9c,13] Although the formation mechanism of nanostructured C_{16}MimCl/boehmite hybrid is not explained clearly, intermolecular interaction between C_{16}MimCl and aluminum hydroxide triggers the hydrolytic transformation process, simultaneously stabilizing the reorganized structure of building blocks as a result of reducing free energy of the crystallites.[9c,14]

Characterization of Physical and Textural Properties of Nanostructured γ-Alumina. TGA curve of C_{16}MimCl/boehmite hybrid indicates that the nanostructured C_{16}MimCl/boehmite hybrid was converted to γ-alumina during calcination in accordance with the elimination of structured water above 100 °C and C_{16}MimCl around 300 °C between the layers of boehmite intercrystallites (see Figure s1 in the Supporting Information). After TGA measurement of γ-alumina up to 900 °C, neither significant weight loss nor demolition of morphology was observed, demonstrating that

(12) Fukushima, T.; Kosaka, A.; Ishimura, Y.; Yamamoto, T.; Takigawa, T.; Ishii, N.; Aida, T. *Science* **2003**, *300*, 2072−2074.

(13) Kuiry, S. C.; Megen, E.; Patil, S. D.; Deshpande, S. A.; Seal, S. *J. Phys. Chem. B* **2005**, *109*, 3868−3872.

(14) (a) Adddachi, M.; Harada, T.; Harada, M. *Langmuir* **1999**, *15*, 7097−7100. (b) Adddachi, M.; Harada, T.; Harada, M. *Langmuir* **2000**, *16*, 2376−2384.

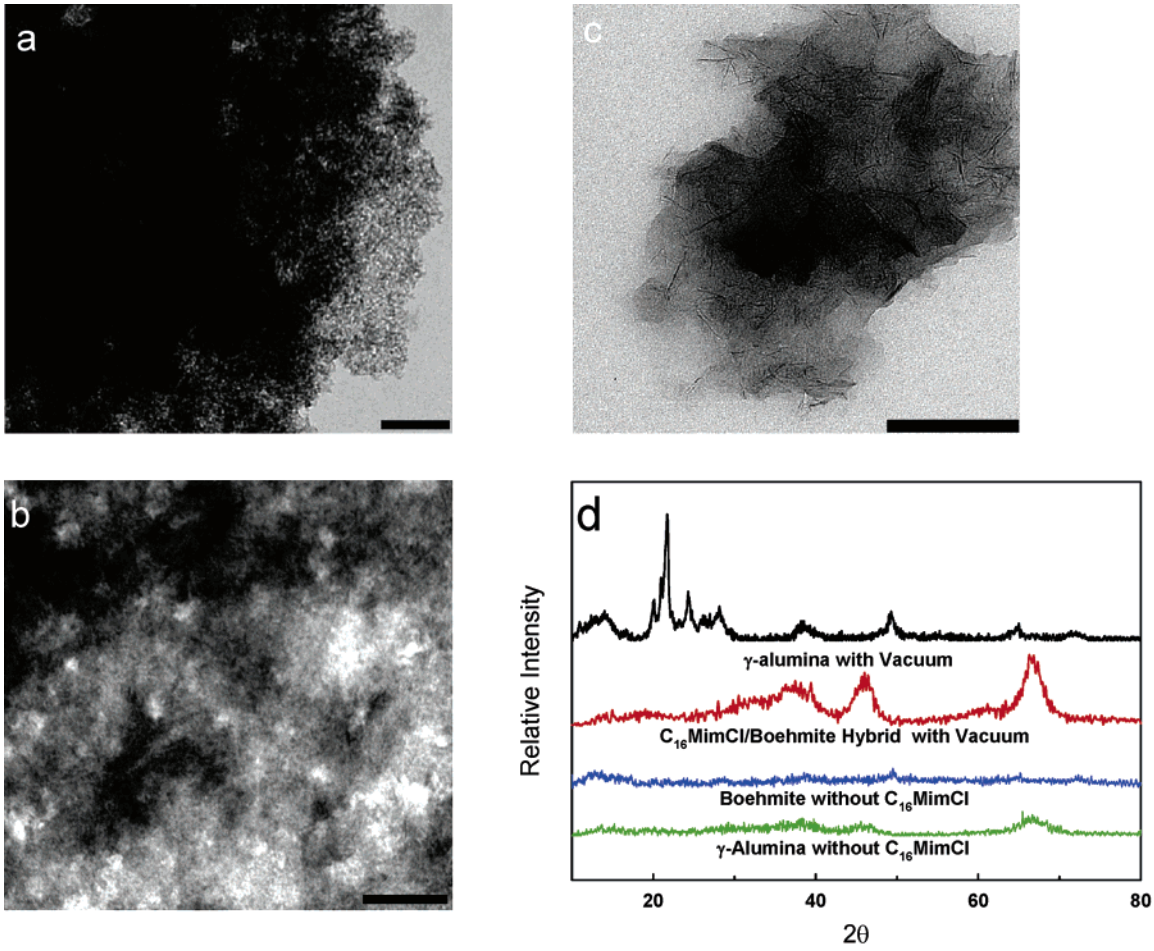

Figure 2. TEM images of (a) γ-alumina without thermal treatment after calcination at 800 °C under the same condition as γ-alumina prepared by C_{16}MimCl (100 nm bar), (b) alumina without C_{16}MimCl after calcination at 800 °C under the same condition as γ-alumina prepared by C_{16}MimCl (200 nm bar), and (c) γ-alumina prepared by C_{16}MimCl after removal of all kinds of volatile solvents by evacuation under vacuum before thermal treatment (100 nm bar). (d) XRD patterns of C_{16}MimCl/boehmite hybrid and γ-alumina after removal of all kinds of volatile solvents by vacuum before thermal treatment and boemite and γ-alumina prepared without C_{16}MimCl under the same condition as γ-alumina prepared by C_{16}MimCl.

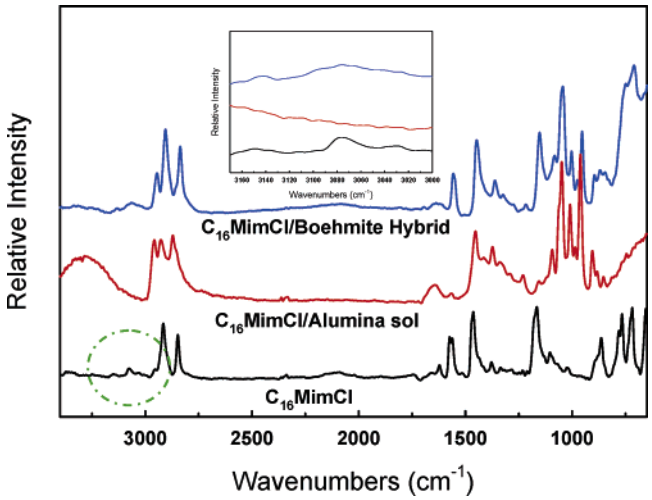

Figure 3. FT-IR spectra of C_{16}MimCl, C_{16}MimCl/aluminum sol, and C_{16}MimCl/boehmite hybrid. Inset is FT-IR spectra in the range of 3000−3170 cm^{-1}.

the nanostructured γ-alumina prepared by C_{16}MimCl had good thermal stability (see Figure s2 in the Supporting Information). C_{16}MimCl was of pivotal importance for inducing the nanostructure of γ-alumina despite the complete removal of C_{16}MimCl above 300 °C, as the key to fabricating γ-alumina was the formation of an intermediate template/boehmite hybrid and the subsequent calcination led to transformation from boehmite to γ-phase with the conservation of morphology of C_{16}MimCl/boehmite hybrid.[5b,d,9c,e] Therefore, the nanostructure of C_{16}MimCl/boehmite hybrid had to be induced in advance of transforming into γ-phase by calcination, to fabricate the nanostructured γ-alumina.

γ-Alumina is a disordered crystalline transitional phase formed through the thermal dehydration of aluminum hydroxides or oxyhydroxides.[5b] Ideally crystalline γ-alumina reveals tetrahedral to octahedral coordinating Al sites in a ratio of 1:3.[9e] ^{27}Al NMR in Figure 4 shows that the nanostructured γ-alumina prepared by C_{16}MimCl was composed of crystalline γ-phase walls because γ-alumina fabricated by calcination at 800 °C revealed tetrahedral to octahedral coordinating Al sites in a ratio of ca. 1:3. Although our γ-alumina did not obtain single crystallinity due to its pristine polycrystalline phase,[5b] XRD peaks, diffused rings in SAED patterns, and ^{27}Al NMR patterns proved the existence of the crystalline γ-phase of the nanostructured alumina. The presence of tetrahedral sites at 65 ppm exhibited nonequivalent Al centers related to acidity of γ-alumina. The existence of tetrahedral and octahedral sites in FT-IR supports the results of ^{27}Al NMR peaks (see Figure s3 in the Supporting Information). The spectrum of γ-alumina shows five bands above 3500 cm^{-1}, which were assigned to

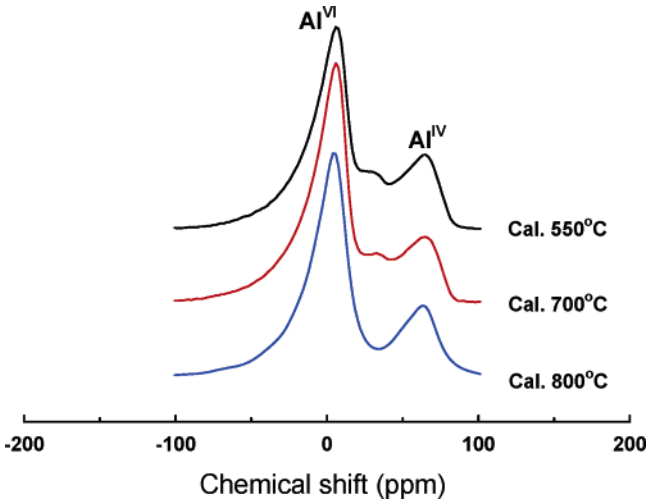

Figure 4. ^{27}Al CP/MAS NMR spectra of γ-aluminas prepared by C_{16}MimCl after calcination at 550, 700, and 800 °C. Peaks around 5, 30, and 65 ppm corresponded to octahedral, pentahedral, and tetrahedral Al sites, respectively.

Table 1. Textural Properties and *d*-Spacing of γ-Aluminas Prepared by C_{16}MimCl after Calcination at 550, 700, and 800 °C

calcination temperature (°C)	surface area[a] ($m^2\ g^{-1}$)	pore size[b] (nm)	pore volume[c] ($cm^3\ g^{-1}$)	*d*-spacing[d] (nm)
550	471.26	9.88	1.46	21.58
700	401.29	10.53	1.42	23.18
800	340.11	11.96	1.37	

[a] Determined by a gas sorption analyzer. Calculated by Brunauer−Emmett−Teller (BET) equation. [b] Determined by a gas sorption analyzer. Calculated by Barret−Joyner−Hallender (BJH) model. [c] Determined by a gas sorption analyzer. [d] Determined by SAXS.

tetrahedral and octahedral coordinated Al species. In particular, pentahedral Al sites at 35 ppm appeared with the decrease in the calcination temperature. Although there is no wide consensus regarding interpretation of this site, it is likely related to the Lewis acidic site in amorphous alumina. This finding indicates that the reduction of amorphous sites resulted from the calcination at higher temperature.

Gas sorption analyzer was used to evaluate the textural property of γ-alumina for the application of catalysts and adsorbents. When the number of pentahedral sites of γ-alumina decreased with the increase of calcination temperature, both surface area and pore volume decreased, while pore size increased as shown in Table 1. The increment of pore size at higher calcination temperature was likely due to the condensation and contraction of pore walls consisting of crystallites via hydrolytic transformation, as described in previous literature.[5c,15] Although the fabricated γ-alumina after calcination at 300 °C obtained good textural properties comparable to those of γ-alumina at 550 °C, transformation of boehmite phase into γ-phase was not accomplished completely (see Figure s4 and Table s1 in the Supporting Information). As a result of that, thermal treatment or calcination above 550 °C was required to condense pore wall and transform crystalline γ-phase. Figure 5 shows that the hysteresis loop of type IV in N_2 sorption/desorption isotherms represented the existence of large mesopores, demonstrating that rodlike or wormlike micelles of C_{16}MimCl formed the cylindrical pores of γ-alumina.[9c] In conventional template synthesis, the pore size of calcined product is strongly related to the molecular size of template. However, no correlation was found between pore size and molecular size of C_{16}MimCl. In a similar manner to SIFF mechanism, it was because C_{16}MimCl was intercalated into the layers of boehmite intercrystallites by means of mutual interaction and existed in wormlike micelles rather than in single molecules.[5c,9c] In addition, Deng and co-workers reported that as the content of ionic liquid increases, the fabricated silica obtains much larger mesopore than the molecular size of the ionic liquid.[10b,c] Interfiber voids formed an irregular porous system due to random distribution of nanofibers and differences in a length and diameter, thereby enhancing the average mesopore size of γ-alumina. Therefore, large mesopores of nanostructured γ-alumina were associated with not only the swelling of micelles as a consequence of large content of C_{16}MimCl but also the origin of fibrious and wormlike morphology. The pore size distribution of a wormlike mesoporous γ-alumina, which was fabricated without thermal treatment under the same condition as γ-alumina prepared by C_{16}MimCl, was narrower than that of a large mesoporous γ-alumina with nanostructure. Thus, the existence of bimodal peaks in pore size distribution was derived from a scaffold structure of γ-alumina consisting of wormlike motif and interfiber voids. Unfortunately, the irregular interfiber voids of γ-alumina widened the pore size distribution due to close range of bimodal peaks, simultaneously increasing the average pore size. Considering the presence of *d* spacing of the SAXS pattern derived from disordered wormlike pores and TEM images of C_{16}MimCl/bohemite hybrid and γ-alumina, the average pore size was determined not by interparticle but by two porous systems consisting of wormlike pores and interfiber voids.

Since the first examples of mesoporous aluminas via supramolecular assembly in 1996,[16] several reports about mesostructured aluminas prepared by solution chemistry were published.[8,17] Despite good textural properties of previous mesostructured aluminas, i.e., large surface area and pore volume, they confront few limits in terms of hydrothermal stability and active sites in catalytic applications due to their pristine amorphous structure. In recent years, after Pinnavaia and co-workers fabricated mesoporous γ-aluminas,[5b,d] solution chemistry such as hydrothermal or template-assisted synthesis was usually used to synthesize the nanostructured γ-alumina.[9c−f,18,19] For the case of hydrothermal synthesis, the fabricated γ-alumina obtained the textural properties with ca. 400−430 m^2/g surface area, ca. 0.7−1.0 cm^3/g pore

(15) (a) Severin, K. G.; Abdel-Fattah, T. M.; Pinnavaia, T. J. *Chem. Commun.* **1998**, 1471−1472. (b) González-Peña, V.; Díaz, I.; Márquez-Alvarez, C.; Sastre, E.; Pérez-Pariente, J. *Microporous Mesoporous Mater.* **2001**, 44−45, 203−210. (c) Li, W. C.; Lu, A. H.; Schmidt, W.; Schuth, F. *Chem. Eur. J.* **2005**, *11*, 1658−1664.

(16) (a) Bagshaw, S. A.; Pinnavaia, T. J. *Angew. Chem., Int. Ed. Engl.* **1996**, *35*, 1102−1105. (b) Vaudry, F.; Khodabandeh, S.; Davis, M. E. *Chem. Mater.* **1996**, *8*, 1451−1464. (c) Yada, M.; Machida, M.; Kijima, T. *Chem. Commun.* **1996**, 769−770.

(17) (a) Yang, P.; Zhao, D.; Margolese, D. I.; Chmelka, B. F.; Stucky, G. D. *Chem. Mater.* **1999**, *11*, 2813−2826. (b) Liu, X.; Wei, Y.; Jin, D.; Shih, W. H. *Mater. Lett.* **2000**, *42*, 143−149.

(18) Zhu, H. Y.; Gao, X. P.; Song, D. Y.; Ringer, S. P.; Xi, Y. X.; Frost, R. L. *Microporous Mesoporous Mater.* **2005**, *85*, 226−233.

(19) Ren, T. Z.; Yuan, Z. Y.; Su, B. L. *Langmuir* **2004**, *20*, 1531−1534.

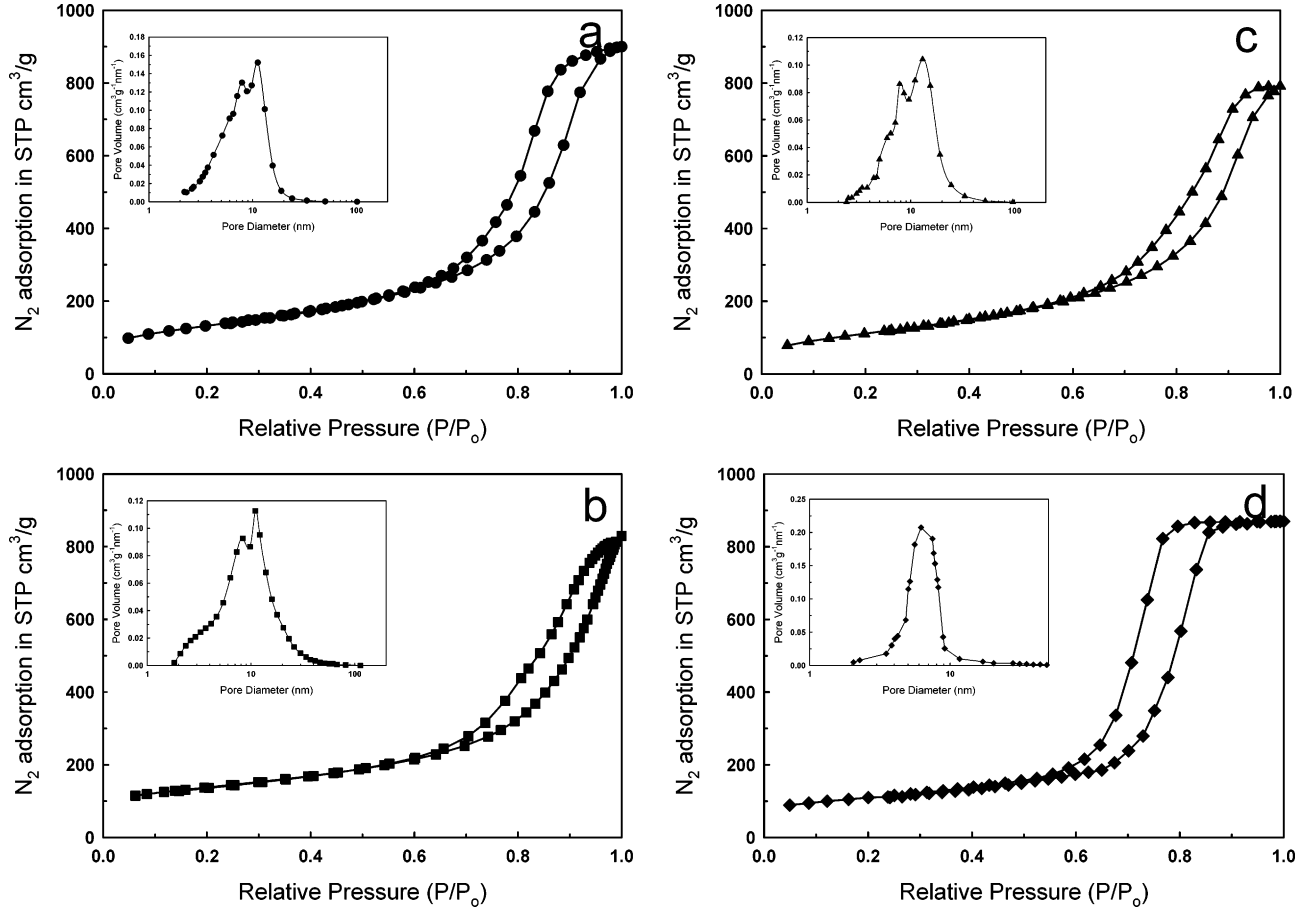

Figure 5. N_2 adsorption/desorption isotherms and pore size distributions of γ-aluminas prepared by C_{16}MimCl after calcination at (a) 550, (b) 700, and (c) 800 °C and (d) N_2 adsorption/desorption isotherms and pore size distribution of γ-alumina fabricated without thermal treatment after calcination at 800 °C under the same condition as γ-alumina prepared by C_{16}MimCl.

volume, and ca. 5−8 nm pore size.[19] For the case of template-assisted synthesis such as surfactant or block copolymer, the nanostructured γ-alumina revealed ca. 300−450 m^2/g surface area, ca. 0.3−1.4 cm^3/g pore volume, and ca. 2−16 nm pore size.[9c−e] In comparison to γ-alumina (surface area of ca. 350−400 m^2/g and pore volume of ca. 1.2−1.4 cm^3/g around 10 nm pore size) reported early as mentioned above, to the best of our knowledge, this γ-alumina with nanostructure obtained the largest surface area and pore volume among large mesoporous γ-aluminas around 10 nm pore size, i.e., 470 $m^2\ g^{-1}$, 1.46 $cm^3\ g^{-1}$, and 9.9 nm after calcination at 550 °C. Therefore, this synthetic method offers new strategy to produce the nanostructured γ-alumina, as it is difficult to form the nanostructure of γ-alumina with satisfactory textural and physical properties due to the difficulty to control the fast rate of reaction compared to silica or titania.

4. Conclusion

In summary, we fabricated a large mesoporous γ-alumina with nanostructure through a thermal process by adjusting dual functions of C_{16}MimCl, i.e., templating and cosolvent functions. In this synthesis, the thermal process with the assistance of RTILs was the key step for induction of the nanostructure of aluminum hydroxide and transformation to boehmite crystallites without the postaddition of organic solvents in an open container at ambient pressure. The formation of a nanostructure and transformation to boehmite crystallites was facilitated by intermolecular interaction between C_{16}MimCl and aluminum hydroxides. FT-IR and XRD verified the presence of hydrogen bonding between anions of C_{16}MimCl and aluminum hydroxides and $\pi-\pi$ stacking of imidazolium rings.

The nanostructures of C_{16}MimCl/boehmite hybrid and γ-alumina were composed of randomly debundled nanofibers embedded in a wormlike porous network as verified by TEM images, SAXS peaks, and bimodal peaks of pore size distribution. Nanofibers revealed a length of ca. 40−60 nm and a diameter of ca. 1.5−3 nm. The existence of crystalline wall of γ-alumina was confirmed by SAED, XRD, and ^{27}Al NMR patterns. As amorphous or pentahedral Al sites of γ-alumina decreased with the increase of calcination temperature indicative of more crystallinity, both surface area and pore volume decreased, while pore size increased. After removal of C_{16}MimCl by calcination, the nanostructured C_{16}-MimCl/boehmite hybrid was converted to γ-alumina without any demolition of morphology. The fabricated γ-alumina displayed better textural properties with ca. 10 nm large mesopore compared to conventional alumina, simultaneously exhibiting good thermal stability and reasonable acidity for the application of catalysts and adsorbents. In particular, a large mesoporous γ-alumina obtained 470 $m^2\ g^{-1}$ in surface area, 1.46 $cm^3\ g^{-1}$ in pore volume, and 9.9 nm in pore size after calcination at 550 °C.

Acknowledgment. This work was financially supported by the Brain Korea 21 (BK21) program and the Advanced Bioseparation Technology Research Center (BSEP, KOSEF). We thank the Korea Basic Science Institute (KBSI) for the use of equipment for TEM and ^{27}Al nuclear magnetic resonance (NMR) measurements.

Supporting Information Available: TGA curves, TEM image, FT-IR spectra, N_2 sorption isotherms and pore size distributions, and table listing textural properties and *d*-spacing. This material is available free of charge via the Internet at http://pubs.acs.org.

CM0620887